METALS AND MATERIALS International, Vol. 8, No. 2 (2002), pp. 191~196

Stress Corrosion Cracking Behavior of Al-Cu-Li-Mg-Zr(-Ag) Alloys

Chang-Soon Lee, Yong Choi and In Gyu Park

Division of Materials and Chemical Engineering, Sun Moon University
100 Galsan-ri, Tangjeong-myun, Asan 336-708, Korea

The effect of aging on the stress corrosion cracking (SCC) behavior of Al-Cu-Li-Mg-Zr(-Ag) alloys such as Weldalite 049 and AA 8090 was studied by the constant elongation test method to investigate their SCC mechanism. The SCC resistance was not very sensitive under the strain rate of 2×10^{-5}/sec, whereas it was significantly decreased under the strain rate of 5×10^{-6}/sec. The SCC preferentially occurred in the intergranular crack mode. The relatively poor SCC resistance of Weldalite 049 in the under-aged condition was improved by aging. Considering the microstructural development during aging, it is related to the dissolution of the precipitation free zone as an anodic area and the strengthening by the coarsening of precipitation.

Keywords : Al-Cu-Li-Mg-Zr(-Ag), stress corrosion cracking (SCC), hydrogen embrittlement (HE), anodic dissolution (AD), precipitate free zone (PFZ)

1. INTRODUCTION

Al-Cu-Li-Mg-Zr(-Ag) alloys have attracted much attention as aerospace materials because of their low density, high elastic constant and high strength. Historically, one of the aluminum alloys, Sceleron (Al-12Zn-3Cu-0.6Mn-0.1Li), was first introduced in 1924 and the commercial high strength aluminum alloys such as 2xxx (Al-Cu-Mg) and 7xxx (Al-Zn-Mg) systems have been used. The three oil crises resulted in stimulating the development of light weight structural materials and the aluminum-lithium alloys have resultantly replaced the conventional aluminum alloys to save energy costs [1,2]. Among these aluminum-lithium alloys, challengeable materials as aerospace materials are Weldalite 049 and AA 8090. Although the alloys show reliable mechanical properties and structural integrity as structural materials, they are restricted in use because of their poor SCC resistance. It is known that pure aluminum, aluminum-manganese, aluminum-silicon, and aluminum-magnesium alloys with a lower level of the elements are not so sensitive to SCC, but other aluminum alloys such as the 2xxx and 7xxx systems are sensitive to it [3,4]. Since the initiation of SCC generally occurs at a local pit formed by a cation [5], such methods as adding alloying elements [6], changing aging conditions [7] and processing treatments [8] to control the microstructure are under extensive study to improve the SCC resistance of Weldalite 049 and AA 8090. In this study, the SCC behavior of the aluminum-copper-lithium alloys was studied by the constant elongation test method. Emphasis is on the effects of aging and the deformation rate on the SCC behavior.

2. EXPERIMENTAL PROCEDURE

The materials used for this study were Al-Cu-Li-Mg-Zr(-Ag) alloys which have recently been developed for aerospace applications, the chemical compositions of which are shown in Table 1.

To control their microstructures and mechanical properties, the specimens were solution treated for 2 hrs at 510°C in a salt bath of KNO_3:$NaNO_3$=1:1 followed by water quenching and aging at 160°C in the same salt bath. The alloys were polished by using alumina powders up to 0.05 μm, and then etched in Keller's solution to observe the microstructure. Micro-vickers hardness was determined under a load of 1000 g and a time of 10~15 sec., and the average value of 7 trials was selected as the measured value of hardness to monitor the aging condition. In addition, an electrochemical corrosion test was carried out in a deaerated aqueous 3.5% NaCl solution (pH=6.7) using a saturated calomel electrode (SCE) and a Pt electrode as a reference electrode and counter electrode, respectively.

Both the mechanical and the stress corrosion tests were carried out using a dynamic test machine (MTS 810) with 25 ton capacity in the strain rate range of 2×10^{-5}~1×10^{-6}/sec at room temperature. Cylindrical tensile specimens were used after being machined parallel to the longitudinal direction according to ASTM G-18 from the extruded plates. The yield strength (YS), tensile strength (UTS) and plastic fracture strain (e_p) were measured from load vs. displacement curves, and fracture energy (E_f) was obtained from the area under the load-displacement curves. The SCC test was performed in

Table 1. Chemical composition of Al-Cu-Li-Mg-Zr(-Ag) alloys (wt.%)

Alloy	Cu	Li	Zr	Mg	Ag	Fe	Si	Ti	Al
Weldalite 049	4.36	1.25	0.14	0.39	0.35	0.07	0.03	0.02	Bal.
AA 8090	1.22	2.40	0.12	0.86	-	0.03	0.05	-	Bal.

3.5% NaCl solution (pH=6.7) under the same strain rates as in air. Because the resistance to stress corrosion is sensitive to surface condition, all the specimens were mechanically polished to remove surface defects introduced during mechanical processing and finally polished using 1.0 μm alumina powder. All the specimens were ultrasonically cleaned in acetone in advance of the stress corrosion test. A corrosion cell 10 cm in diameter and 4 cm high was made of transparent cylindrical acryl to observe specimen failure. 3.5% NaCl solution was used as a corrosion solution, circulated continuously with a pump to prevent its pH change. Fracture surfaces of the specimens after the tests were observed by scanning electron microscopy (Jeol 6400) to identify the fracture behavior according to strain rate and aging treatment.

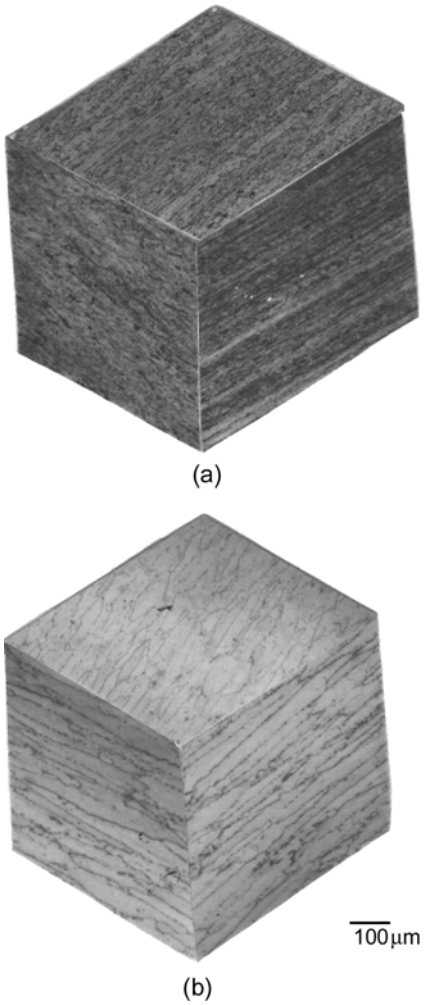

Fig. 1. Three dimensional optical micrographs of as-received Al-Cu-Li alloys: (a) Weldalite 049 and (b) AA 8090.

3. RESULTS

Fig. 1 shows the three dimensional optical micrographs of Al-Cu-Li alloys. The microstructures consist of pancake type grains with anisotropy and macroscopic delamination in the thickness direction. Fig. 2 shows the hardness change with aging time. Weldalite 049 reached the maximum hardness value after 50 hrs aging, but AA 8090 did not even after 120 hrs aging.

Table 2 shows the result of the tensile test with Weldalite 049 in air. Weldalite 049 showed higher YS and UTS at 50 hrs than at 10 hrs of aging, and showed a variation with strain rates.

The polarization curves of each alloy with aging condition obtained from corrosion tests carried out in a corrosive environment of 3.5% NaCl solution are shown in Fig. 3, and the

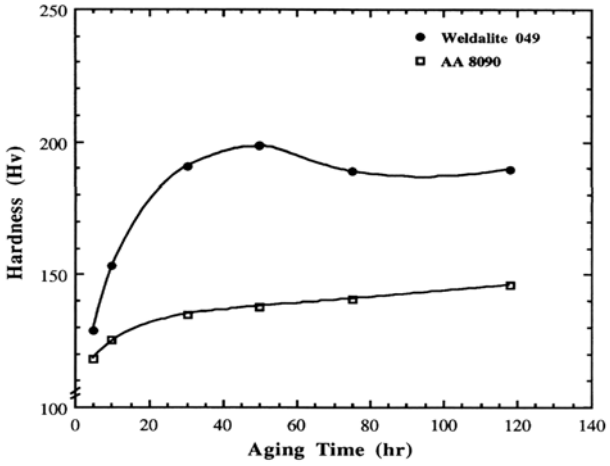

Fig. 2. Aging curves of Al-Cu-Li alloys.

Table 2. Tensile properties of Weldalite 049 in air

Strain Rate (/sec)	Aging Time (hr)	YS (MPa)	UTS (MPa)	e_p (%)
2×10^{-5}	10	439	545	15.6
	50	550	611	10.8
5×10^{-6}	10	367	531	22.8
	50	447	572	15.1
1×10^{-6}	10	338	512	23.7
	50	424	539	16.3

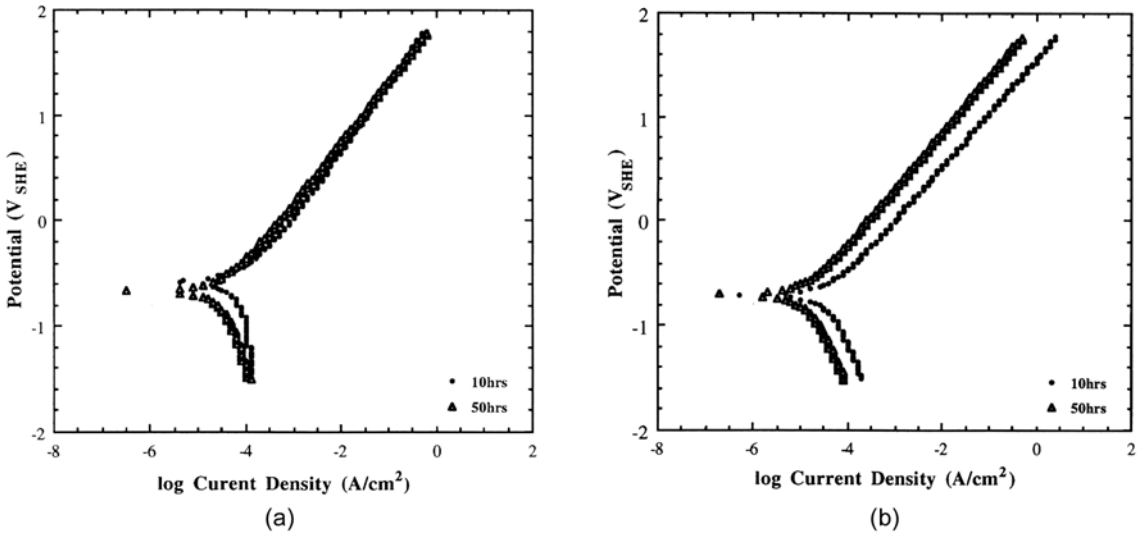

Fig. 3. Polarization curves of Al-Cu-Li alloys in 3.5% NaCl solution (pH=6.7): (a) Weldalite 049 and (b) AA 8090.

Table 3. Corrosion potential and corrosion rate of Al-Cu-Li alloys

Alloy	Aging Time (hr)	E_{corr} (mV_{SHE})	I_{corr} (A/cm^2)	E_{oc} (mV_{SHE})
Weldalite 049	10	-657.8	7.482×10^{-6}	-677.43
	50	-702.9	4.076×10^{-5}	-708.86
AA 8090	10	-709.6	4.227×10^{-5}	-711.40
	50	-702.4	1.445×10^{-5}	-702.20

Table 4. Tensile properties of Weldalite 049 in 3.5% NaCl

Strain Rate (/sec)	Aging Time (hr)	YS (MPa)	UTS (MPa)	e_p (%)	E_{scc}/E_{air} (%)	$E_{scc}/E_{air}\|_{(anode)}$ (%)
2×10^{-5}	10	372	535	13.4	100	-
	50	442	569	8.6	100	-
5×10^{-6}	10	358	506	16.2	66.29	11.99
	50	434	533	12.4	84.57	22.73
1×10^{-6}	10	313	483	17.7	53.66	-
	50	413	498	12.7	78.15	-

result is summarized in Table 3. Corrosion rates of the alloys and the corrosion potential of Weldalite 049 decreased with aging, but that of AA 8090 was almost the same.

A stress corrosion test was carried out in 3.5% NaCl (pH=6.7) solution to see the resistance of the alloys aged for 10 and 50 hrs to stress corrosion. Mechanical properties and the change in fracture energy with aging time and strain rate are summarized in Tables 4 and 5 for Weldalite 049 and AA 8090, respectively. YS and UTS increased as aging time increased with little difference when compared with those in air, especially in the case of 50 hrs of aging. AA 8090 showed the same trend as Weldalite 049, and the SCC resulted in 10~20% of reduction in fracture strain in both alloys.

The ratio of the fracture energy of Weldalite 049 in air and 3.5% NaCl solution (E_{scc}/E_{air}) is compared in Fig. 4 with strain rate, and the resistance to SCC decreased with decreasing strain rate. The strain rate dependence of SCC in under aged and peak aged conditions showed that the ratio of fracture energy becomes 1 under a strain rate as fast as 2×10^{-5}/sec, which is thought it is failure mainly by mechanical deforma-

Table 5. Tensile properties of AA 8090 in 3.5% NaCl at strain rate of 5×10^{-6}/sec

Aging Time (hr)	YS (MPa)	UTS (MPa)	e_p (%)	E_{scc}/E_{air} (%)	$E_{scc}/E_{air}\|_{(anode)}$ (%)
10	323	448	16.3	84.64	12.94
50	361	477	10.03	82.88	12.92

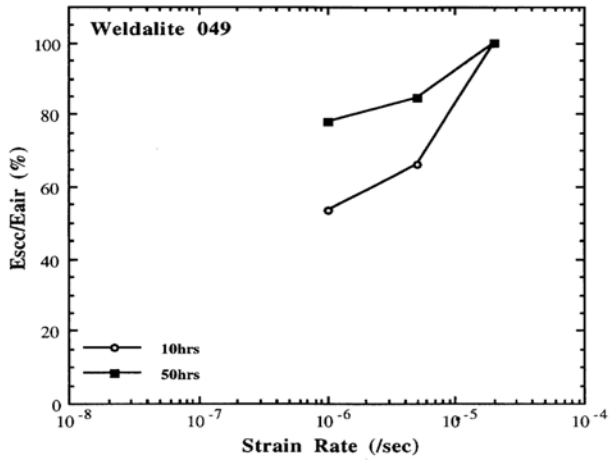

Fig. 4. Comparison of fracture energy of Weldalite 049 in accordance with strain rate.

tion and SCC was observed at lower strain rates.

In order to see the effect of corrosion potential on the stress corrosion rate the stress corrosion test was carried out under the strain rate of 5×10^{-6}/sec after polarization to ±100 mV from the free corrosion potential. When no potential was applied, the free corrosion potentials of Weldalite 049 were -657.8 mV_{SHE} and -702.9 mV_{SHE} for 10 hrs and 50 hrs of aging conditions, respectively, while those of AA 8090 were -709.6 mV_{SHE} and -702.4 mV_{SHE} for 10 hrs and 50 hrs of aging conditions, respectively. When two alloys were anodically polarized to +100 mV from the free corrosion potential, anodic dissolution was accelerated and thus increased stress corrosion resulted in rapid failure. As shown in Tables 4 and 5, the reduced resistance to SCC under anodic polarization decreased the fracture energy to below 20% of that in air. Weldalite 049 showed less resistance to SCC when aged for 10 hrs than 50 hrs, a result similar to that in the free corrosion potential. Aging treatment for 10 hrs resulted in higher resistance to SCC in AA 8090 than in Weldalite 049, and the treatment for 50 hrs in AA 8090 showed less resistance to SCC than it did at 10 hrs, similar to Weldalite 049. AA 8090 was shown to be less sensitive to anodic polarization than Weldalite 049.

The fracture modes of the two alloys were identified by observing the fracture surfaces under SEM as shown in Fig. 5. Weldalite 049 showed intergranular fracture which is a typical fracture appearance in Al alloys, but AA 8090 showed a fibrous appearance which is typical in materials with a highly deformed orientation. Optical micrographs showing microcracks around the fracture surface are shown in Fig. 6. Microcracks were shown to propagate along grain boundaries, implying that the fracture mode of the two alloys was a typical intergranular fracture.

4. DISCUSSION

Fig. 2 shows the aging curves of Weldalite 049 and AA 8090 alloys. It is interesting why Weldalite 049 easily reaches the peak aging condition, but AA 8090 does not. The hardness change is influenced by microstructural development, especially nucleation and growth of precipitation. Tosten *et al.* [9] measured the volume fraction of precipitates with aging in Al-Cu-Li, and reported that the volume fraction of the δ' phase decreased with aging time from the beginning stage. The driving force of the nucleation and growth of the precipitation is related to energy restored by cold working and alloying elements. As shown in Fig. 1, Weldalite 049 has a more heavily deformed structure than AA 8090 and seems to reach peak aging after 50 hrs, whereas AA 8090 does not even after 120 hrs. This kind of microstructure will show different corrosion and mechanical properties. As shown in Table 3, the corrosion rate and corrosion potential of Weldalite 049 significantly decreased with aging; however, the corrosion rate of AA 8090 slightly decreased and the cor-

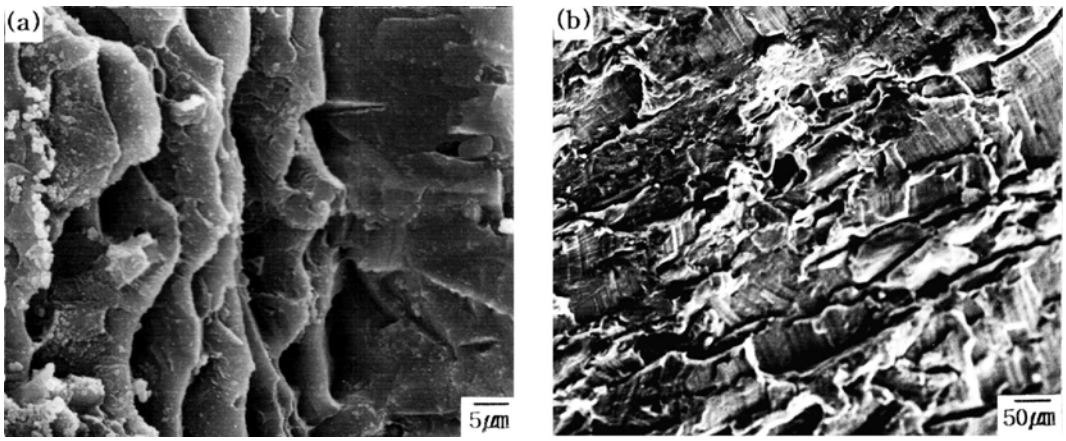

Fig. 5. SEM fractographs of Al-Cu-Li alloys strained at 1×10^{-6}/sec: (a) Weldalite 049 and (b) AA 8090.

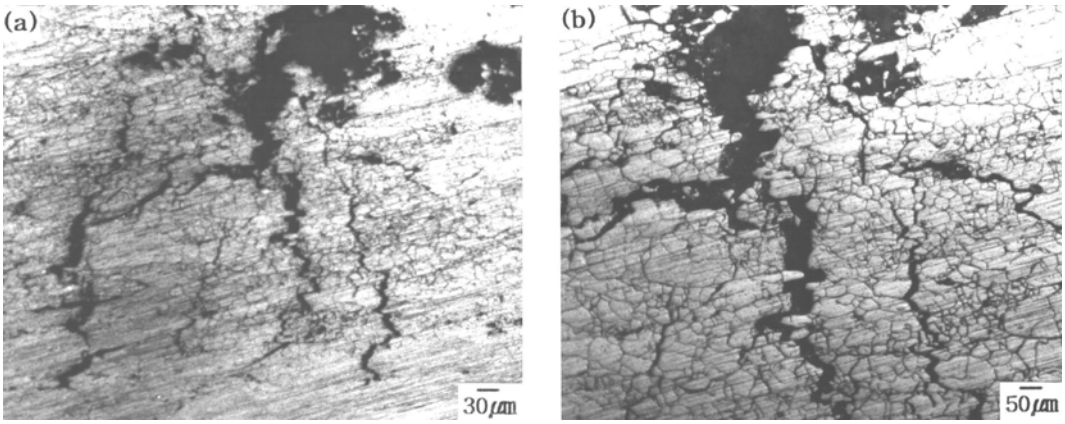

Fig. 6. Microcracks of Al-Cu-Li alloys around the fracture surface (3.5% NaCl, pH=6.7): (a) Weldalite 049 and (b) AA 8090.

rosion potential of AA 8090 was almost the same. The different corrosion behaviors of the two alloys are also related to their microstructures. It is difficult to observe the change of the amount of δ' phase in this study, but it is expected that Weldalite 049 after 50 hrs aging will have relatively wide PFZ and coarse precipitates, whereas AA 8090 will have a similar microstructure even after 50 hrs aging. Considering the chemistry of PFZ and precipitates, they tend to act as anode and cathode, respectively. The corrosion behavior depends on the surface condition in the electrolytic solution. In this study, the electrolytic solution contains enough chloride ions to effectively make pits on the aluminum alloys. Accordingly, the ions can selectively attack passive films on the anodic area such as the PFZ and the corrosion potential of Weldalite 049 was significantly decreased; however, that of AA 8090 was not. Besides, corrosion rates, of course, are related to the kinetic behavior of ionic dissolution and depend much more on the relative size of anodic and cathodic areas. It is difficult to determine the anodic and the cathodic areas based on the metallurgical point of view. However, it is expected that the area effect on corrosion behavior will be more effectively observed on the specimen under peak- and over-aged conditions. Hence, Weldalite 049 and AA 8090 showed different corrosion behaviors after 50 hrs aging.

As shown in Table 5, the stress corrosion resistance of AA 8090 expressed by the fracture energy ratio in a corrosive environment and air showed similar values of about 84.64% and 82.88% under open potential, and 12.94% and 12.92% under 100 mV_{SHE} anodic potential for 10 and 50 hrs of aging, respectively. This also supports the hypothesis that the microstructure of AA 8090 did not significantly change after 50 hrs aging. Since the stress corrosion resistance of Weldalite 049 under the aging condition in equal test conditions showed 66.29%, AA 8090 has more SCC resistance than Weldalite 049 under the aging condition although Weldalite 049 has higher YS and UTS than AA 8090. This may be related to as-received conditions and the alloying elements of the alloys.

The SCC resistance of Weldalite 049 after 50 hrs aging is higher than that of under-aged AA 8090. The YS and UTS of Weldalite 049 and AA 8090 measured in a corrosive environment and air at 5×10^{-6}/sec also increased with aging time, as shown in Tables 4 and 5, respectively. One of interesting points in Weldalite 049 is that its SCC resistance improved from 66.29% to 84.57% under open potential and from 11.99% to 22.73% under 100 mV_{SHE} anodic potential after 50 hrs aging. The SCC behavior of Weldalite 049 after 50 hrs aging showed different SCC behavior from that of AA 8090 under anodic potential. The anodic potential enhances pit formation and anodic dissolution on the surface. In the case of Weldalite 049, the possible anodic area such as the PFZ becomes wider after 50 hrs aging and the corrosion rate increased about one order as shown in Table 3. This means that the improved SCC resistance of Weldalite 049 after 50 hrs aging is related more to the increased mechanical properties due to the formation of precipitation than to the increased anodic area due to the formation of PFZ.

In order to study the SCC mechanism more precisely, the strain rate effect of the alloys was determined. As shown in Fig. 4, the SCC resistance of Weldalite 049 decreased with decreasing strain rates. The SCC resistance of Weldalite 049 after 10 hrs aging changed from 66.29% for 5×10^{-6}/sec to 53.66% for 1×10^{-6}/sec, whereas the SCC resistance of Weldalite 049 after 50 hrs aging changed from 84.57% for 5×10^{-6}/sec to 78.15% for 1×10^{-6}/sec. The reduced strain rate retards the dislocation generation, moving and passive film break and enhances the pit formation time and corrosion. The reduction rates of the SCC resistance of Weldalite 049 after 10 hr and 50 hr agings were about 19% and 7%, respectively.

In this study, cathodic polarization by -100 mV_{SHE} caused less than 5% difference in fracture energy from that by air. During cathodic polarization, cathodic potential causes hydrogen evolution and decreases the anodic dissolution rate. It is

difficult to find the hydrogen embrittlement which usually occurs during cathodic polarization in this study, but the decrease in the anodic dissolution rate by cathodic polarization is thought to have caused mechanical failure.

According to Pugh *et al.* [10] local pitting at the PFZ, which acts as an anode to the matrix in corrosive environments, causes micro-cracks, and the stress concentration in the soft area causes the fracture of protective films through plastic deformation, and the re-corrosion of bare metals exposed by fracture causes the propagation of cracks. Accordingly, it is expected that Weldalite 049 will follow the formation of a pit by the typical anodic dissolution. One of characteristics of the constant elongation test method used in this study accelerates crack initiation and propagation by breaking passive film due to the extrusion of dislocation and bare metal to surface. The dislocations in the peak-aged specimen are not moved well in the matrix by the precipitates but are in PFZ. The important role of the subgrain T_1 (Al_2CuLi) phase in pitting and SCC behavior has been proposed in many studies [11], and the dissolution of the T_1 phase was a general factor in most of the proposed mechanisms. The corrosion potential of the T_1 phase, which is the main strengthening phase in Al-Cu-Li alloys, is -0.854 mV_{SHE} (0.6 M NaCl), and is thought to have high resistance to stress corrosion in terms of the corrosion potential difference with the matrix. Reboul and Meyer [12] showed that an addition of Li in Cu-containing alloys increased intergranular corrosion. The T_1 phase, which has a higher strengthening effect than δ' and nucleates homogeneously during the early stage of aging, is thought to have a close relationship to resistance to stress corrosion in Weldalite 049 with a higher Cu/Li ratio, but AA 8090, with a lower Cu/Li ratio, did not show much difference in resistance to stress corrosion with aging time. AA 8090 showed lower mechanical properties than Weldalite 049 under the same aging condition, but the resistance to stress corrosion compared in terms of fracture energy was similar after 50 hrs of aging and was higher after 10 hrs of aging. This is thought to come from the Cu/Li ratio, the volume fraction of precipitates according to alloying elements and composition, and the difference in the microstructure of the two alloys.

The decrease of fracture energy and rapid failure during anodic dissolution are thought to come from a decrease in the effective area by pitting at the surface due to a higher free corrosion potential than pitting potential. The surface of the specimen was black after the stress corrosion test and many pittings were observed at the surface. The combined effect of the increased anodic dissolution rate during anodic polarization and decrease of the effective area by pitting at the surface is thought to have accelerated the stress corrosion cracking. Hence, the aging and strain effects on the SCC of Weldaite 049 observed in this study support the hypothesis that the SCC mechanism is related to a mechano-electrochemical model involving the pit formation at the PFZ and precipitates for strengthening.

5. CONCLUSIONS

The following conclusions were obtained through a characterization of the SCC behavior of two Al-Cu-Li alloys with aging treatment using a constant elongation test method.

(1) Weldalite 049 has lower SCC resistance than AA 8090 under aging conditions although the former has higher YS and UTS.

(2) The SCC resistance of Weldalite 049 after 50 hrs aging is higher than that of under-aged AA 8090. The improved SCC resistance of Weldalite 049 is more related to the increased mechanical properties due to the formation of precipitates than the increased anodic area due to the formation of the PFZ.

(3) The aging and strain effects on the SCC of Weldalite 049 observed in this study support the hypothesis that the SCC mechanism is related to a mechano-electrochemical model involving the pit formation at the PFZ and precipitates for strengthening.

REFERENCES

1. D. S. Chung, S. J. Lee and H. K. Cho, *J. Kor. Inst. Met. & Mater.* **34**, 1601 (1996).
2. K. H. Lee, S. G. Cho, S. W. Lee and Y. J. Lee, *J. Kor. Inst. Met. & Mater.* **34**, 552 (1996).
3. A. Conde, B. J. Fernandez and J. J. de Damborenea, *Corros. Sci.* **40**, 91 (1988).
4. Y. Choi, S. I. Pyun and H. C. Kim, *J. Mater. Sci.* **19**, 1517 (1984).
5. R. J. Kilmer and G. E. Stoner, *Scripta metall.* **25**, 243 (1991).
6. G. M. Ludka and D. E. Laughlin, *Metall. Trans. A* **12**, 2083 (1981).
7. J. K. Thompson, E. S. Tankin and V. S. Agarwala, *Materials Performance,* p. 45, NACE (1987).
8. K. G. Kent, *J. Aust. Inst. Met.* **15**, 171 (1970).
9. M. H. Tosten, A. K. Vasudevan and P. R. Howell, *Metall. Trans. A* **19**, 51 (1988).
10. E. N. Pugh and W. R. K. Jones, *Metallurgica* **63**, 3 (1961).
11. J. G. Rinker, M. Marek and T. H. Sanders, Jr., *Al-Li Alloys*, p. 597, TMS-AIME, Warrendale, PA (1984).
12. M. Revoul and P. Meyer, *Aluminum-Lithium*, p. 881, TMS-AIME, Warrendale, PA (1987).